Catal Lett (2013) 143:23–30
DOI 10.1007/s10562-012-0935-9

Catalytic Conversion of Ethanol into Butanol over M–Mg–Al Mixed Oxide Catalysts (M = Pd, Ag, Mn, Fe, Cu, Sm, Yb) Obtained from LDH Precursors

Ioan-Cezar Marcu · Nathalie Tanchoux · François Fajula · Didier Tichit

Received: 21 July 2012 / Accepted: 27 October 2012 / Published online: 27 November 2012

Abstract Ethanol conversion into butanol was performed over MMgAlO mixed oxide catalysts (M = Pd, Ag, Mn, Fe, Cu Sm, Yb). The highest butanol yields were obtained with the Pd-containing mixed oxide, which exhibited a remarkable stability during the reaction. A good correlation was found between the amount of basic sites of medium and high strength and the selectivity to butanol.

Keywords Mixed oxide catalysts · Hydrotalcites · Ethanol · Butanol

1 Introduction

The conversion of ethanol into 1-butanol is of particular industrial interest. 1-Butanol is indeed a crucial building block for acrylic acid and acrylic esters and is widely used as a solvent or as an additive to gasoline [1–4]. The potential use of bioethanol as a raw material could also allow obtaining convenience products coming from renewable resources widely available throughout the world.

Therefore, the Guerbet reaction, which corresponds to the catalytic transformation of light alcohols into higher ones, e.g. of ethanol into 1-butanol, attracts more and more interest. Several studies of the Guerbet reaction in liquid phase have shown that a basic catalyst is needed along with dehydrogenating/hydrogenating functions [5–9]. Several homogeneous or heterogeneous catalysts or mixtures of catalysts have been tested which usually associate basic properties with transition metals such as Ni, Ru or Rh [5–17]. Layered double hydroxides (LDHs) were shown as very promising precursors for the preparation of such catalysts acting either as basic catalysts which were then combined with copper chromite [15], or directly as precursors of bifunctional mixed oxide catalysts by introducing metal cations in the structure [12]. These catalysts were efficient in the Guerbet condensation of methanol with *n*-propanol. However, several types of transition or lanthanide metal cations are able to modify the basic and dehydrogenating/hydrogenating functions in the catalysts obtained from multicationic LDH and probably in different manner depending on the alcohol.

In this paper the synthesis of 1-butanol from ethanol over M–Mg–Al (with M = Pd, Ag, Mn, Fe, Cu, Sm, Yb) mixed oxide based catalysts obtained from LDH precursors has been performed. We investigated particularly by TPD of CO_2 and NH_3 experiments the influence of the nature of the metal cation on the equilibrium between acid and basic functions, and then on the catalytic performances.

I.-C. Marcu · N. Tanchoux (✉) · F. Fajula · D. Tichit
Institut Charles Gerhardt, UMR 5253 CNRS/ENSCM/UM2/UM1, Matériaux Avancés pour la Catalyse et la Santé (MACS), Ecole Nationale Supérieure de Chimie, 8, rue de L'Ecole Normale, 34296 Montpellier Cedex 5, France
e-mail: nathalie.tanchoux@enscm.fr

Present Address:
I.-C. Marcu
Laboratory of Chemical Technology & Catalysis, Department of Organic Chemistry, Biochemistry and Catalysis, Faculty of Chemistry, University of Bucharest, 4-12, Blv. Regina Elisabeta, 030018 Bucharest, Romania

2 Experimental

2.1 Catalysts Preparation

LDH precursors were prepared by coprecipitation at constant pH ($\approx$10) of suitable amounts of $Mg(NO_3)_2{\cdot}6H_2O$ and $Al(NO_3)_3{\cdot}9H_2O$ (Mg/Al = 3) with a solution of NaOH

(2 M) into a well-stirred beaker containing 200 mL of a solution of suitable amount of different metal nitrate solutions $M(NO_3)_n{\cdot}xH_2O$ (M/(M + Mg + Al) = 0.05) where M = Pd, Ag, Mn, Fe, Cu, Sm, Yb. The addition of the alkaline solution and the pH were controlled by pH-STAT Titrino (Metrohm). The precipitates formed were aged in their mother liquor overnight at 353 K under stirring, separated by centrifugation, washed with deionized water until a pH of 7 was reached and dried at 353 K overnight. The samples were noted M5MgAlOH, where 5 is the metal content as atomic percent with respect to the cations.

The previous dried samples were calcined in flowing nitrogen at 823 K during 8 h in order to form the corresponding mixed metal oxides catalysts. They were noted M5MgAlO.

2.2 Catalysts Characterization

The textural characterization was achieved using conventional nitrogen adsorption/desorption method, with a Micromeritics ASAP 2010 automatic analyzer. Prior to nitrogen adsorption, the samples were outgassed for 8 h at 523 K.

Powder X-ray diffraction (XRD) patterns were obtained using a Siemens D5000 Diffractometer and monochromatic Cu Kα radiation. They were recorded with 0.02° (2) steps over the 3°–70° angular range with 1 s counting time per step.

The thermal analysis (TG and DTG) was carried out using a Netzsch TG 209 device, in the following conditions: linear heating rate 10 K min^{-1}. from room temperature to 1,173 K, dynamic air atmosphere, Al_2O_3 crucible, sample weight approximately 20 mg.

Temperature-programmed desorption (TPD) of CO_2 and NH_3 were carried out using a Micromeritics Autochem model 2910 instrument. Fresh calcined samples (100 mg) were pretreated in air at 823 K before adsorption of the probe molecules at 373 K. During desorption, the sample was heated in a helium flow (30 mL min^{-1}) at a ramp of 10 K min^{-1}. The amount of the probe molecules desorbed from the sample was estimated from the area under the peak after taking the thermal conductivity detector response into consideration.

Characterization of the samples has been performed before and, for some of them, after the catalytic test.

2.3 Catalytic Reaction

The catalytic performances of the various catalysts were evaluated by means of experiments with 50 mL (39.5 g) ethanol (Riedel-de Haën, 99.8 %) conducted in a 100 mL steel autoclave at 473 K or in the range 473–533 K and autogenic pressure under stirring. Unless specified, each run was carried out over a period of 5 h using 0.5 g of catalyst activated at 823 K. The reaction products were analyzed by gas chromatography (HP 4890D, equipped with a DB-1 capillary column and a flame ionization detector), and the response factors related to decane as external standard were determined for ethanol and the products which were identified with pure commercial samples. The predominant reaction products were *n*-butanol, 1,1-diethoxyethane, acetaldehyde, ethyl acetate, butyraldehyde, 1,1-diethoxybutane, crotonaldehyde, methyl ethyl ketone and diethyl ether. The carbon and oxygen mass balances, based on the products listed, were always higher than 92 % and, in most of the cases, higher than 95 %.

3 Results and Discussion

3.1 Catalysts Characterization

Catalysts textural properties, obtained by nitrogen adsorption at 77 K, are summarized in Table 1. The specific surface areas of the samples were in the range from 166 to 213 $m^2\ g^{-1}$. All materials displayed type IV nitrogen adsorption/desorption isotherms with a distinct hysteresis loop, characteristic of mesoporous materials. The absence of micropores in these materials was ascertained by the analysis of the t-plots derived from the sorption isotherms. After the catalytic reaction, the specific surface areas of the samples remained practically the same (Table 1).

The XRD patterns of the as-prepared precursors and final catalysts are displayed in Figs. 1 and 2, respectively. Poorly crystallized hydrotalcite-type structures were detected on all dried as-prepared samples. The basal spacing corresponding to the (003) reflection of ca. 8 Å, was in agreement with the presence of nitrates as compensating anions [18]. Pd5MgAlOH, Ag5MgAlOH and Sm5MgAlOH samples, displayed diffraction peaks corresponding to poorly crystallized PdO (JCPDS 41-1107),

Table 1 Catalysts textural properties, obtained by nitrogen adsorption at 77 K

Catalyst	Specific surface area ($m^2\ g^{-1}$)		Pore volume (mL g^{-1})
	Before reaction	After reaction	
Pd5MgAlO	187	189	0.20
Ag5MgAlO	166	–	0.23
Mn5MgAlO	167	163	0.22
Fe5MgAlO	213	–	0.25
Cu5MgAlO	180	–	0.23
Sm5MgAlO	187	187	0.39
Yb5MgAlO	183	–	0.74

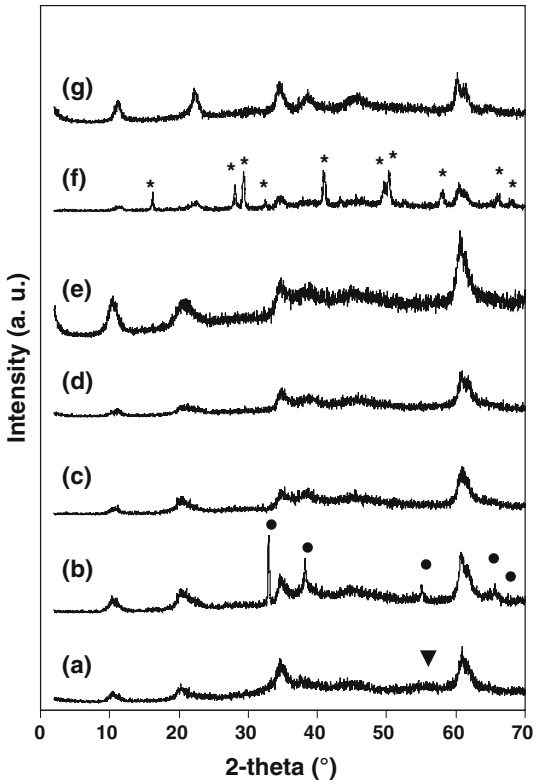

Fig. 1 XRD patterns of the LDH precursors. *a* Pd5MgAlOH. *b* Ag5MgAlOH. *c* Mn5MgAlOH. *d* Fe5MgAlOH. *e* Cu5MgAlOH. *f* Sm5MgAlOH. *g* Yb5MgAlOH (*black down pointing triangle* PdO, *black circle* Ag_2O, *asterisk* $Sm(OH)_3$)

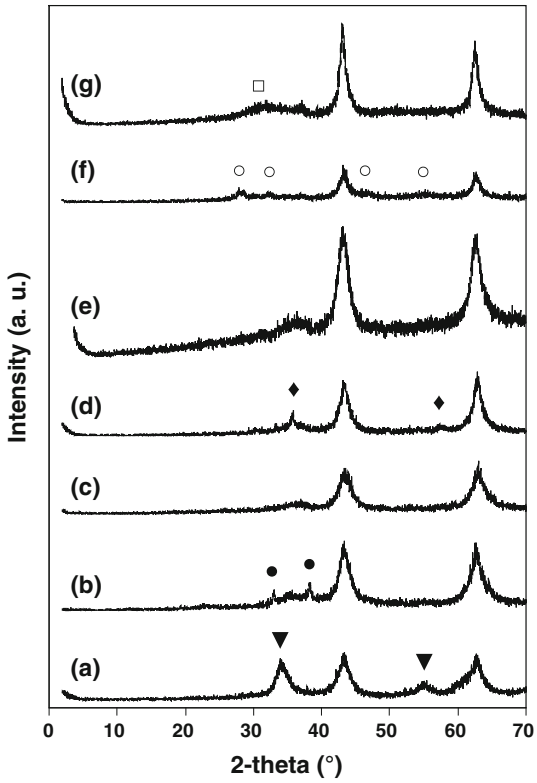

Fig. 2 XRD patterns of the mixed-oxide catalysts after calcination at 823 K. *a* Pd5MgAlO. *b* Ag5MgAlO. *c* Mn5MgAlO. *d* Fe5MgAlO. *e* Cu5MgAlO. *f* Sm5MgAlO. *g* Yb5MgAlO (*black down pointing triangle* PdO; *black circle* Ag_2O, *black diamond suit* $FeAl_2O_4$,*white circle* Sm_2O_3, *white square* Yb_2O_3)

Ag_2O (JCPDS 75-1532) and $Sm(OH)_3$ (JCPDS 83-2036) phases, respectively. Samples calcined at 823 K exhibited, in all cases, the characteristic peaks of the MgAlO mixed oxide corresponding to the salt rock-like structure (JCPDS-ICDD 4-0829), as a major phase. Lines corresponding to PdO, Ag_2O, $FeAl_2O_4$ (JCPDS 34-0192), Sm_2O_3 (JCPDS 15-0813) and Yb_2O_3 (JCPDS 41-1106) were also detected for the Pd, Ag, Fe, Sm and Yb-containing mixed oxide catalysts, respectively. XRD patterns of the samples remained practically unchanged after reaction, in line with the observed stability of the surface areas.

The TG-DTG curves of the Sm5MgAlOH precursor and of the corresponding Sm5MgAlO mixed oxide, representative of all samples and given as example are presented in Fig. 3. The first weight loss below 473 K in the TG curves of the LDH precursor was due to the removal of loosely bound and interlayer water molecules. The second weight loss giving an intense DTG peak at 675 K was ascribed to the removal of the hydroxyl groups of the brucite-like layers and to the decomposition of the compensating nitrate anions. The sample exhibited a total weight loss of 43 % up to 1,073 K, with the second weight loss being larger than the first one. This general behavior is in agreement with literature data for hydrotalcite-like materials [19–21]. The TG curves of the calcined samples also showed two weight losses. The first one gives rise to two maxima in the DTG peak which can be assigned to the departure of two types of adsorbed water molecules differently bounded. The second weight loss was probably due to the removal of water and/or adsorbed carbonates resulting from a slight rehydroxylation and carbonation of the mixed oxide in contact with air. However, the total weight loss in Sm5MgAlO reaching 23 % is almost two times smaller than in Sm5MgAlOH. This confirmed the large range of irreversible dehydroxylation in this latter sample.

It is well known that the MgAlO mixed oxides obtained via thermal decomposition of Mg/Al LDH precursors possess several sorts of active sites [22–25]. Weak Brønsted basic sites are associated with surface OH^- groups remaining few after activation; medium-strength Lewis sites are related to $Mg^{2-}O^{2-}$ and Al^{3+}–O^{2-} acid–base pairs; while strong Lewis basic sites are due to the presence of low coordinated O^{2-}. Moreover, when transition, noble or lanthanide M^{n+} cations are introduced in the mixed oxide structure or when an excess oxide phase of these cations is present, M^{n+}–O^{2-} acid–base pairs are obviously also present. These different sorts of acid–base Lewis pairs are generally the major species in the materials. The equilibrium

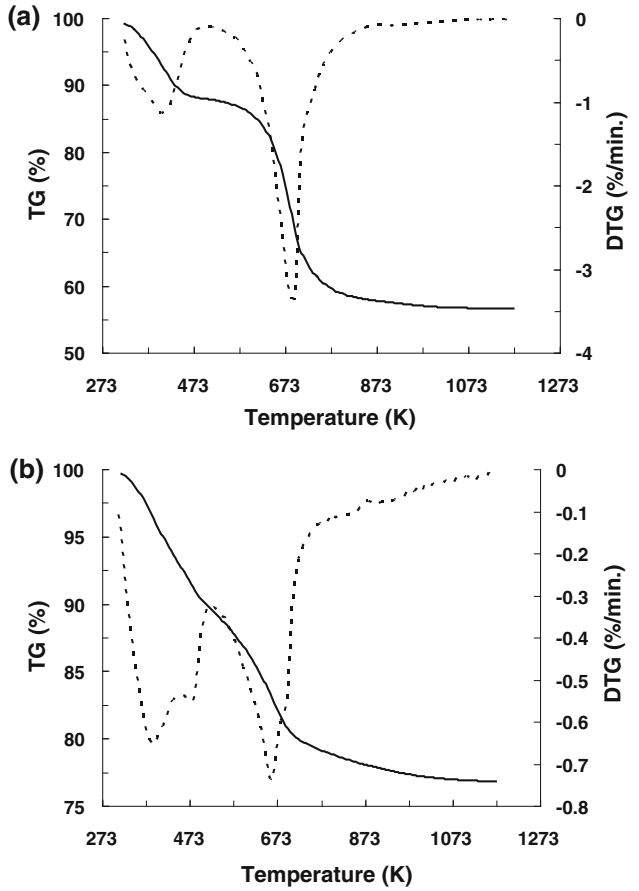

Fig. 3 TG-DTG profiles of uncalcined Sm5MgAlOH precursor (**a**) and of the resulting Sm5MgAlO mixed oxide (**b**)

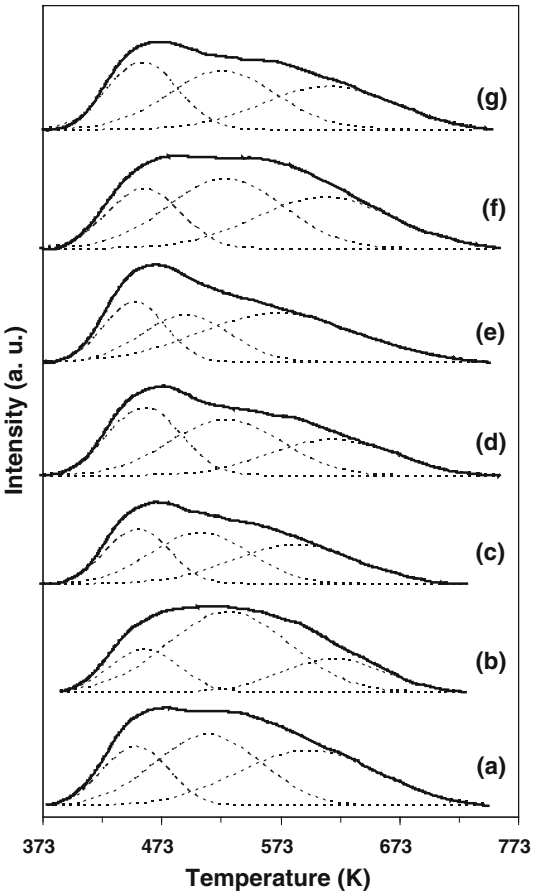

Fig. 4 CO_2-TPD profiles of the mixed-oxide catalysts. *a* Pd5MgAlO. *b* Ag5MgAlO. *c* Mn5MgAlO. *d* Fe5MgAlO. *e* Cu5MgAlO. *f* Sm5MgAlO. *g* Yb5MgAlO

between Lewis acid and base sites is therefore expected to vary on one hand upon introduction of M^{n+} metal cations in the structure, and on the other hand in function of the M^{n+} cations involved because of their different electronegativity. These variations are the key point explaining the catalytic behavior of the different samples. In order to confirm this assessment, the number and strength of basic and acid sites of the materials were investigated by CO_2 and NH_3-TPD, respectively.

CO_2-TPD profiles of the catalysts studied are shown in Fig. 4. These very broad profiles extending from 373 to 773 K were deconvoluted in three desorption peaks with maxima at about 450, 520 and 590 K, accounting for the presence of sites of weak (W), medium (M) and high (H) basic strength, respectively. The amount of CO_2 desorbed in these peaks allowed to calculate the number of sites reported in Table 2. All samples mainly exhibited sites of medium and high strength. These sites are in similar amount in Pd5MgAlO, Mn5MgAlO, Sm5MgAlO and Yb5MgAlO, while sites of medium strength were the major ones in Ag5MgAlO and those of high strength the major ones in Cu5MgAlO. Regarding the total number of sites, the highest was observed for the Pd- and Sm-containing mixed oxides and the lowest for the Mn-containing one.

NH_3-TPD profiles of the catalysts studied are shown in Fig. 5. As in the case of the CO_2-TPD profiles, they were deconvoluted in three peaks with maxima at 461–483, 520–587 and 600–663 K corresponding to acid sites exhibiting weak (W), medium (M) and high strength (H), respectively. Their amounts were reported in Table 3. Both the total number and the relative amount of sites of different strength showed a different behavior than for the basic sites for the different mixed oxides. The largest variations in the total number of acid sites were indeed observed with a twofold increase from Mn5MgAlO and Fe5MgAlO with respect to Sm5MgAlO and Yb5MgAlO. In these latter samples, this was due to the very low amount of sites of high strength. The sites of medium strength were the major ones in all the mixed oxides.

From these results of CO_2 and NH_3-TPD experiments one can emphasize the general tendencies observed. The

Table 2 Number of basic sites of different strength for mixed oxides, derived from TPD of CO_2

Catalyst	CO_2 desorbed (mmol g^{-1})			Total basicity (mmol CO_2 g^{-1})
	W	M	H	
Pd5MgAlO	0.39	0.76	0.79	1.94
Ag5MgAlO	0.29	0.98	0.35	1.62
Mn5MgAlO	0.35	0.52	0.49	1.36
Fe5MgAlO	0.50	0.64	0.46	1.60
Cu5MgAlO	0.37	0.42	0.79	1.58
Sm5MgAlO	0.44	0.82	0.71	1.97
Yb5MgAlO	0.47	0.64	0.57	1.68

Table 3 Number of acid sites of different strength for mixed oxides, derived from TPD of NH_3

Catalyst	NH_3 desorbed (mmol g^{-1})			Total acidity (mmol NH_3 g^{-1})
	W	M	H	
Pd5MgAlO	0.30	0.96	0.48	1.74
Ag5MgAlO	0.48	1.08	0.78	2.34
Mn5MgAlO	0.66	1.47	1.24	3.37
Fe5MgAlO	1.06	1.67	0.78	3.51
Cu5MgAlO	0.62	0.99	0.69	2.30
Sm5MgAlO	0.52	0.89	0.10	1.51
Yb5MgAlO	0.62	0.67	0.25	1.54

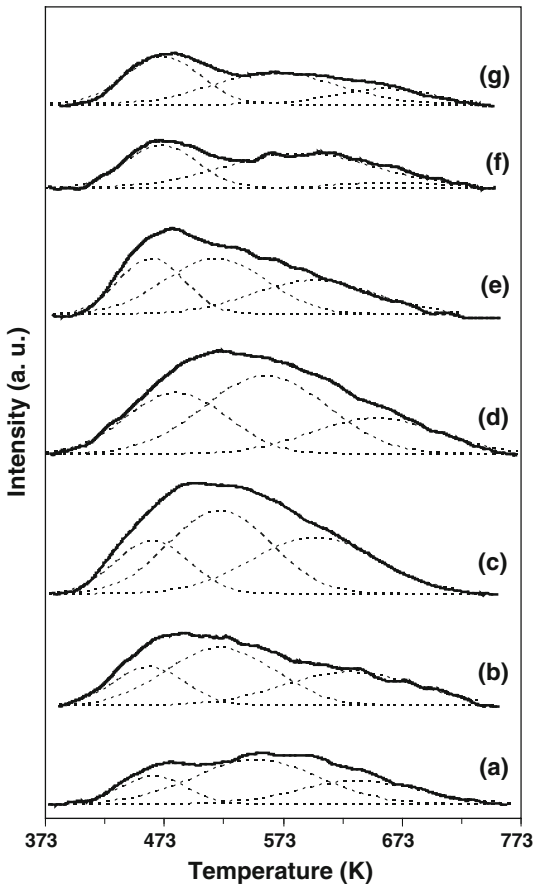

Fig. 5 NH_3-TPD profiles of the mixed-oxide catalysts. *a* Pd5MgAlO. *b* Ag5MgAlO. *c* Mn5MgAlO. *d* Fe5MgAlO. *e* Cu5MgAlO. *f* Sm5MgAlO. *g* Yb5MgAlO

acid character was the most pronounced in Mn5MgAlO, Fe5MgAlO, Ag5MgAlO and Cu5MgAlO which possess the highest total number of sites, and particularly a high proportion of sites of medium and high strength while, on the other hand, the amount of basic sites was the lowest. Sm5MgAlO and Pd5MgAlO exhibited a slightly higher basic character than the other mixed oxides.

3.2 Catalytic Study

The seven M5MgAlO catalysts (M = Pd, Ag, Mn, Fe, Cu, Sm, Yb) prepared were evaluated in ethanol conversion, the obtained results being presented in Table 4. The intrinsic activity expressed as the overall rate of the catalytic reaction within the reactor normalized by the surface area of the catalyst within the reactor at 5 h reaction time as well as the space–time butanol yield defined as the number per unit time of moles of butanol made per unit surface of catalyst were also calculated and presented in Table 4. We observe that the ethanol conversion varied between 0.3 % for Fe based catalyst and 4.1 % for Cu based catalyst. Obviously, the catalytic activity depends on the acido-basic properties of the catalysts related to the nature of the metal M. In all cases butanol was the main reaction product. Cu and Pd-based catalysts were the most active both in terms of conversion and intrinsic activity, but the former gave both butanol and 1,1-diethoxyethane as main products, while the later was quite selective to butanol. Note that they have similar concentrations of strong basic sites, but Cu5MgAlO has a higher concentration of strong acid sites as well as a higher total acidity. Sm5MgAlO is also highly selective to butanol which is in agreement with its similar total concentration and distribution of basic sites of different strength than Pd5MgAlO. However, Sm5MgAlO is less active than Pd5MgAlO, suggesting that the equilibrium between basic and acid sites is better achieved in the case of Pd5MgAlO. The same conversion was reached with Yb5MgAlO and Sm5MgAlO but the former was less selective to butanol according, as previously suggested for the other samples, to its lower basic character. Fe5MgAlO and Mn5MgAlO which were amongst the most acid catalysts, were poorly active and highly selective to 1,1-diethoxyethane and acetaldehyde. Ag5MgAlO which has the lowest concentration of strong basic sites gave the lowest selectivity to butanol and a high selectivity to ethyl acetate. These results confirmed that the

Table 4 Ethanol conversion and product selectivities over M5MgAlO catalytic systems

Catalyst	Conv. (%)	Selectivities (%)								Intrinsic activity (10^9 mol m^{-2} s^{-1})	Butanol STY (10^9 mol m^{-2} s^{-1})
		Acetal C6	Acetal C8	Ethanal	Butanal	Crotonal	Butanol	EA	DET		
Pd5MgAlO	3.8	2.5	1.0	12.3	7.0	–	72.7	4.0	0.6	19.9	14.5
Ag5MgAlO	1.6	7.5	1.3	17.5	5.6	3.3	38.8	25.9	–	9.2	3.6
Mn5MgAlO	0.7	6.9	5.0	21.0	4.1	6.8	53.3	2.9	–	4.0	2.1
Fe5MgAlO	0.3	26.7	2.4	21.7	–	7.1	39.2	2.7	–	1.3	0.5
Cu5MgAlO	4.1	35.9	5.1	9.9	1.7	0.2	40.3	6.9	–	21.7	8.8
Sm5MgAlO	1.3	6.6	1.2	15.1	4.0	3.6	66.3	3.1	–	6.6	4.4
Yb5MgAlO	1.2	15.1	3.7	19.1	2.7	2.3	53.0	4.1	–	6.3	3.3

Reaction conditions: 473 K, 5 h

Acetal C6 1,1-diethoxyethane, *Acetal C8* 1,1-diethoxybutane, *Ethanal* acetaldehyde, *Butanal* butyraldehyde, *Crotonal* crotonaldehyde, *EA* ethyl acetate, *DET* diethyl ether, *STY* space–time yield

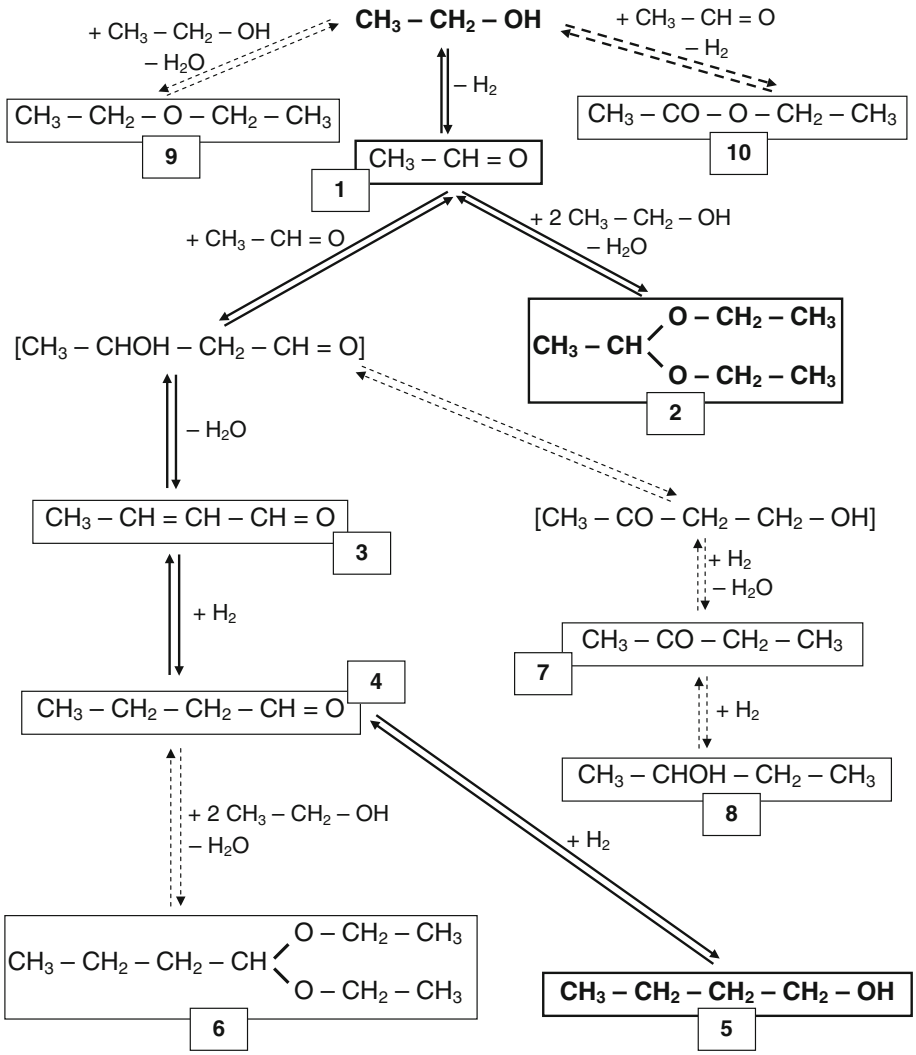

Fig. 6 Reaction scheme for ethanol transformation on M–MgAlO catalysts [15]. The observed products are presented in a frame. The *continuous line arrows* show the two main pathways leading to the two main products: 1-butanol and 1,1-diethoxyethane. The *dotted line arrows* show the secondary pathways of the ethanol reaction. (1) Acetaldehyde; (2) 1,1-diethoxyethane; (3) crotonaldehyde; (4) butyraldehyde; (5) 1-butanol; (6) 1,1-diethoxybutane; (7) methyl ethyl ketone; (8) 2-butanol; (9) diethyl ether; (10) ethyl acetate

equilibrium between the acid and basic functions of the mixed oxides determine the activity and the selectivity in the reaction of conversion of ethanol. The selectivity for *n*-butanol increased when the number of strong basic sites increased. This suggests that acetaldehyde self-condensation, catalyzed by the basic sites, would be the rate

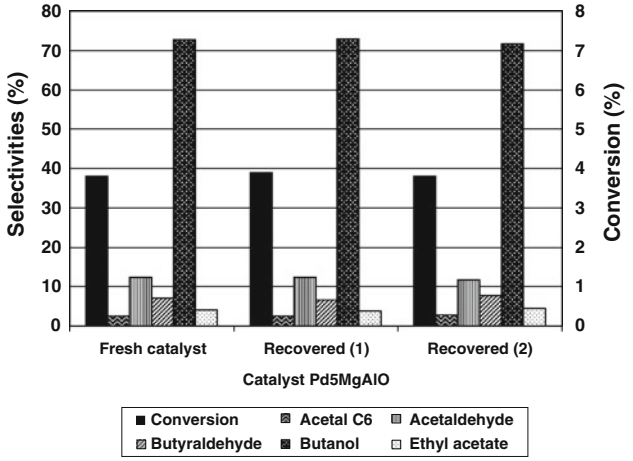

Fig. 7 Activity of the Pd5MgAlO system for three successive runs. Reaction conditions: 473 K, 5 h reaction time

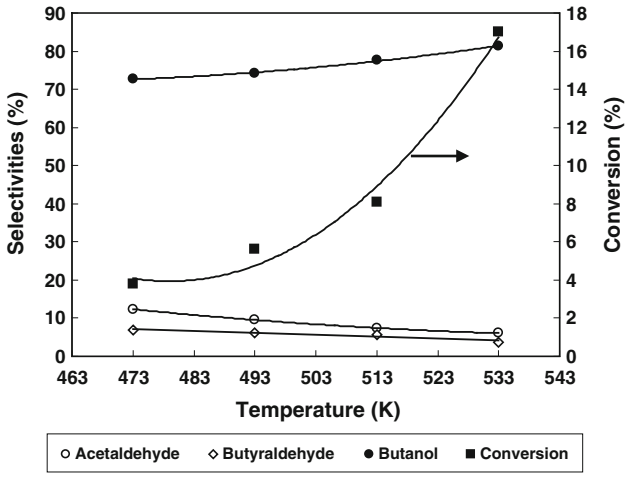

Fig. 8 Variation of the total conversion of ethanol and of the selectivities as a function of the reaction temperature for the Pd5MgAlO catalytic system. Reaction time: 5 h

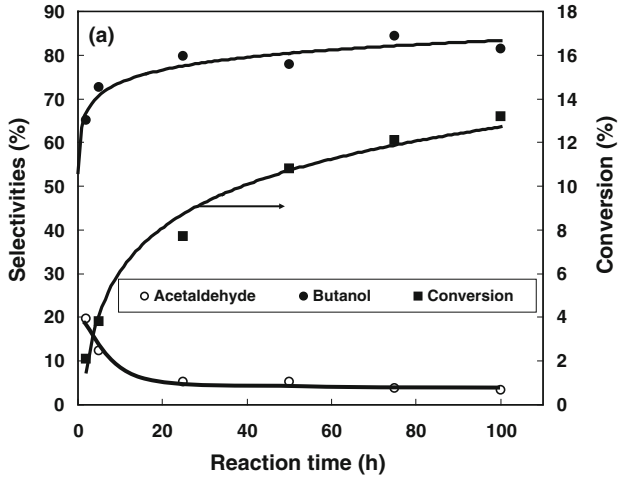

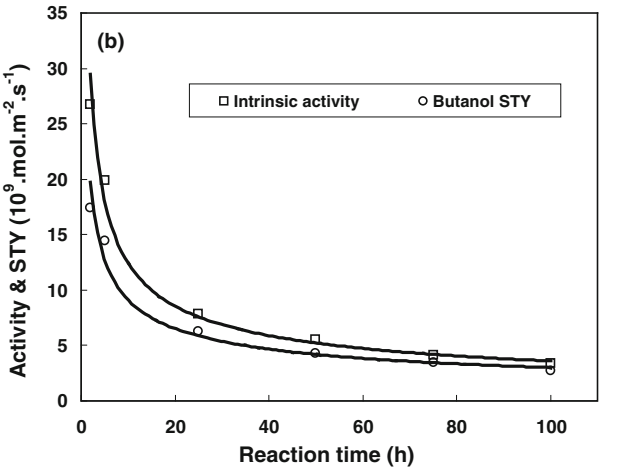

Fig. 9 Effect of the reaction time on the catalytic properties of Pd5MgAlO: **a** Evolution with time of conversion and selectivities. **b** Evolution with time of intrinsic activity and space–time butanol yield. Reaction temperature: 473 K

determining step of the transformation of ethanol into butanol. The acid properties of the catalysts play an important role in the formation of the other products. These results confirm the reaction pathways already proposed for the ethanol transformation over Cu–Mg–Al oxides [16] and presented in Fig. 6.

The Pd based catalyst being the most selective for butanol, was more extensively studied. Firstly, we checked the stability of Pd5MgAlO calcined at 823 K. Three successive reactions were carried out with the same catalyst recovered between each run by filtration and dried overnight at 523 K. The results obtained are shown in Fig. 7. Because the conversion and the product distribution remained strictly the same, we can consider that the catalytic properties are stable at least during three successive reactions.

Figure 8 shows the variations of the total conversion of ethanol and selectivities to main reaction products with the reaction temperature in the range 473–533 K. As expected, the conversion increased with the reaction temperature from ~4 % at 473 K to 17 % at 533 K. At the same time, the selectivity for butanol increased up to 81 % at the expense of acetaldehyde and butyraldehyde.

When the reaction time was varied from 2 to 100 h, the ethanol conversion increased from 2.1 to 13.2 % and the selectivity for butanol increased from 65 to 81.5 % (Fig. 9a) still at the expense of acetaldehyde and butyraldehyde. At the same time, the intrinsic activities of the catalyst as well as the space–time yield (STY) of butanol follow typical curves as a function of time as shown in Fig. 9b.

Water which is a by-product of the reaction (see Fig. 6) can influence the structure of the catalysts due to the well known memory effect of the Mg(Al)O mixed oxide obtained from LDH precursor. Presence of water is also

Table 5 Effect of water addition to the reactant on the catalytic properties of the Pd-based catalyst

Reaction conditions	Conv. (%)	Selectivities (%)						
		Acetal C6	Acetal C8	Ethanal	Butanal	Butanol	EA	DET
With pure ethanol	3.8	2.5	1.0	12.3	7.0	72.7	4.0	0.6
With ethanol 96 %	3.0	9.5	7.6	18.5	11.4	48.2	4.9	–

Reaction temperature: 473 K. Reaction time: 5 h

Acetal C6 1,1-diethoxyethane, *Acetal C8* 1,1-diethoxybutane, *Ethanal* acetaldehyde, *Butanal* butyraldehyde, *EA* ethyl acetate, *DET* diethyl ether

able to modify the nature of the active sites from Lewis to Brønsted type. Therefore the influence of the addition of water to ethanol was investigated in this work with the most active Pd5MgAlO catalyst. As reported in Table 5, only a slight decrease of conversion was observed whereas selectivities to acetals, acetaldehyde and butyraldehyde were increased at the expense of that to butanol.

4 Conclusion

Ethanol conversion into butanol was performed over MMgAlO mixed oxide catalysts (M = Pd, Ag, Mn, Fe, Cu Sm, Yb). The nature of the cations modifies the equilibrium between the acid and basic functions and thus determine the catalytic performances. The better equilibrium allowing reaching the highest butanol yield was obtained with the Pd-containing mixed oxide. A good correlation was found between the amount of basic sites of medium and high strength and the selectivity to butanol. On the other hand, the presence of a large amount of acid sites increases the selectivity to 1,1-diethoxyethane and acetaldehyde. The addition of water to the reaction mixture has a detrimental influence on the selectivity to butanol. The catalysts exhibited a remarkable stability during the reaction.

Acknowledgments The authors are grateful to Mr. Thomas Cacciaguerra for his expert technical assistance with XRD experiments. This work was performed under the frame of ANR BioEdiesel ANR-06-BLAN-0005.

References

1. Di Cosimo JI, Apesteguia CR, Gines MJL, Iglesia E (2000) J Catal 190:261
2. Gines MJL, Iglesia E (1998) J Catal 176:155
3. Hilmen AM, Xu M, Gines MJL, Iglesia E (1998) Appl Catal A 169:355
4. Kirk RE, Othmer DF (1978) Encyclopedia of chemical technology, vol 4, 3rd edn. Wiley, New York, p 338
5. Gregorio G, Pregaglia GF, Ugo R (1972) J Organomet Chem 37:385
6. Burk PL, Pruett RL, Campo KS (1985) J Mol Catal 33:15
7. Miller R, Bennett G (1961) Producing 2-ethylhexanol by the Guerbet reaction. Ind Eng Chem 53:33–36
8. Carlini C, Di GM, Marchionna M, Noviello M, Raspolli GAM, Sbrana G (2002) J Mol Catal A 184:273
9. Carlini C, Di Girolamo M, Macinai A, Marchionna M, Noviello M, Raspolli Galletti AM, Sbrana G (2003) J Mol Catal A 200:137
10. Carlini C, Macinai A, Marchionna M, Noviello M, Galletti AMR, Sbrana G (2003) J Mol Catal A 206:409
11. Carlini C, Macinai A, Raspolli Galletti AM, Sbrana G (2004) J Mol Catal A 212:65
12. Carlini C, Marchionna M, Noviello M, Raspolli Galletti AM, Sbrana G, Basile F, Vaccari A (2005) J Mol Catal A 232:13
13. Pruett RL, Young DA, Duncan CB, Mozeleski EJ (1989) EP Patent 299720A2
14. Wick A, Mahnke EU (2011) WO Patent 2011054483A1
15. Carlini C, Flego C, Marchionna M, Noviello M, Raspolli GAM, Sbrana G, Basile F, Vaccari A (2004) J Mol Catal A 220:215
16. Marcu IC, Tichit D, Fajula F, Tanchoux N (2009) Catal Today 147:231
17. Ndou AS, Plint N, Coville NJ (2003) Appl Catal A 251:337
18. Rives V, Ulibarri MA (1999) Coord Chem Rev 181:61
19. Das J, Das D, Parida KM (2006) J Colloid Interface Sci 301:569
20. Tichit D, Das N, Coq B, Durand R (2002) Chem Mater 14:1530
21. Parida KM, Das J (2000) J Mol Catal A 151:185
22. Diez VK, Apesteguia CR, Di Cosimo JI (2000) Catal Today 63:53
23. Corma A, Fornes V, Martin-Aranda MR, Rey F (1992) J Catal 134:58
24. Di Cosimo JI, Diez VK, Xu M, Iglesia E, Apesteguia CR (1998) J Catal 178:499
25. Prinetto F, Ghiotti G, Durand R, Tichit D (2000) J Phys Chem B 104:11117